Supporting Information

Self-Passivation of LiNiO$_2$ Cathode for Lithium-Ion Battery through Zr Doping

Chong S. Yoon,[†] Un-Hyuck Kim,[‡] Geon-Tae Park,[‡] Suk Jun Kim,[‖] Kwang-Ho Kim,[§] Jaekook Kim,[⊥] and Yang-Kook Sun*[‡]

[†]Department of Materials Science and Engineering, Hanyang University, Seoul 04763, South Korea

[‡]Department of Energy Engineering, Hanyang University, Seoul 04763, South Korea

[‖] School of Energy, Materials, and Chemical Engineering, Korea University of Technology and Education (KOREATECH), Cheonan 31253, South Korea

[§]School of Materials Science and Engineering, Pusan National University, Busan 46241, South Korea

[⊥] Department of Materials Science and Engineering, Chonnam National University, Gwangju 61186, South Korea

Corresponding Author

E–mail: yksun@hanyang.ac.kr (Y.-K. Sun)

EXPERIMENTAL METHODS

Material synthesis: A spherical Zr-doped $Ni(OH)_2$ precursor was synthesized by co-precipitation of aqueous $NiSO_4 \cdot 6H_2O$ and $Zr(SO_4)_2 \cdot 4H_2O$ solutions (molar ratio of Ni:Zr of 98.6:1.4). The mixed solution was continuously pumped into a batch reactor (47 L) filled with deionized water, NaOH(aq), and NH_4OH(aq) under a nitrogen atmosphere with vigorous stirring. Concurrently, a 4.0-mol·L^{-1} NaOH solution (aq) and NH_4OH chelating-agent solution (aq) were pumped separately into the reactor.[1] Zr-doped $Ni(OH)_2$ precursor powder was obtained through filtration, washing, and vacuum drying at 110 °C for 12 h. The precursor powder was mixed with $LiOH \cdot H_2O$ (Li:Ni = 1.01:1) and calcined at 650 °C for 10 h under a high-purity oxygen atmosphere.

Analytical techniques: The chemical compositions of the prepared powders were determined by inductively coupled plasma (ICP-OES, OPIMA 8300, Perkin Elmer). The crystalline phase was analyzed by powder and electrode XRD (Empyrean, Panalyitical) using Cu K_α radiation. XRD data were obtained in a 2θ range of 10° to 110° at a speed of 0.02°·min^{-1}. The structural refinement was performed by a Rietveld analysis using the Fullprof suite.[2] The morphologies and structures of the prepared particles were observed by TEM (JEOL 2010, JEOL). The TEM samples were prepared by focused ion-beam milling (FIB, NOVA 200/ FEI).

Electrochemical Testing: For the fabrication of positive electrodes and 2032-coin-type half-cell testing, the synthesized powders were mixed with carbon black (super-P:KS-6 = 4:6 wt%) and polyvinylidene fluoride (PVDF, Solef 5130) (90:5.5:4.5 wt%) in N-methylpyrrolidinone. The obtained slurry was coated on an Al foil, roll-pressed, and vacuum-dried. The electrolyte solution was 1.2 M $LiPF_6$ in ethylene-carbonate–ethyl-methyl-carbonate (EC:EMC = 3:7 (vol.%)) with 2 wt% vinylene carbonate (VC) (PanaX Etec, Korea). Preliminary cell tests were performed with a 2032-coin-type half-cell using lithium metal as the anode. The cells were charged and discharged by applying a constant current

density of 90 mA·g^{-1} (0.5 C-rate) at 30 °C between 2.7 V and 4.3 V versus Li$^+$/Li. An electrochemical impedance spectroscopy analysis was performed after charging to 4.3 V versus Li$^+$/Li as a function of the number of cycles with a multi-channel potentiostat (Bio-Logic, VMP3) from 1 MHz to 1 mHz.

Thermal analysis: For a DSC analysis, the 2032-coin-type cells were fully charged to 4.3 V and opened in an Ar-filled glove box. Once the remaining electrolyte was removed using dimethyl carbonate, the washed cathode material was scraped from the current collector. A stainless-steel sealed pan with a gold-plated copper seal was used to contain 7.0 mg of the sample with the electrolyte. Measurements were performed using a DSC 200 PC (NETZSCH) at a temperature scan rate of 5 °C·min^{-1}.
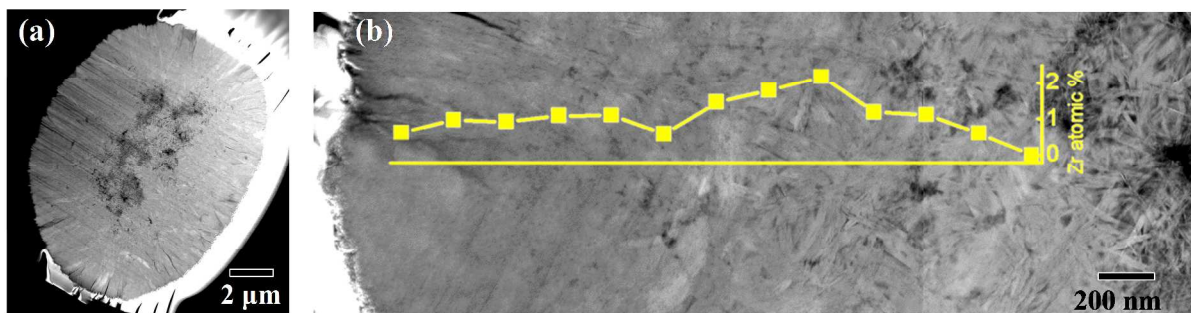
Figure S1. (a) Cross-sectional scanning transmission electron microscopy (STEM) dark-field image of the Zr-doped $Ni(OH)_2$ and (b) mosaic image of a conventional bright-field TEM image with an energy dispersive x-ray spectroscopy (EDS) profile of Zr along the radial direction of the particle.
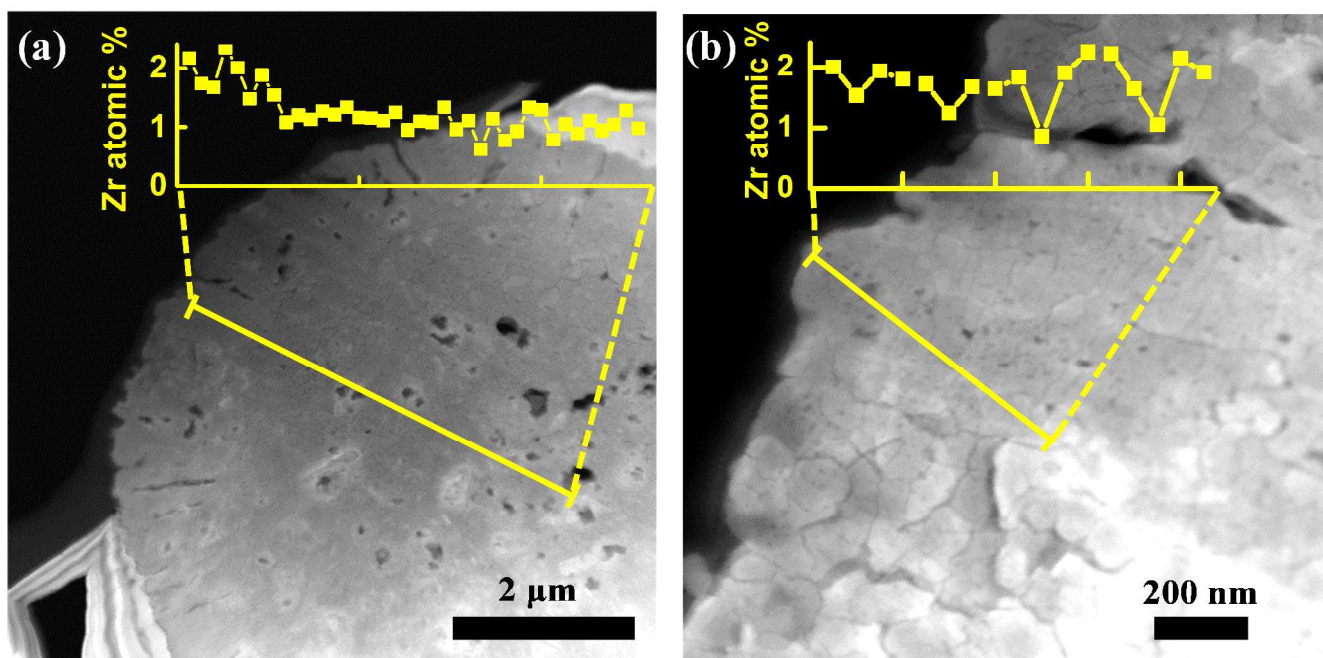
Figure S2. (a) Cross-sectional scanning transmission electron microscopy (STEM) dark field image of the Zr doped $LiNiO_2$ with an EDS profile of Zr along the radial direction of the particle. and (b) surface morphology and an EDS profile of Zr along the radial direction of the local particle surface.
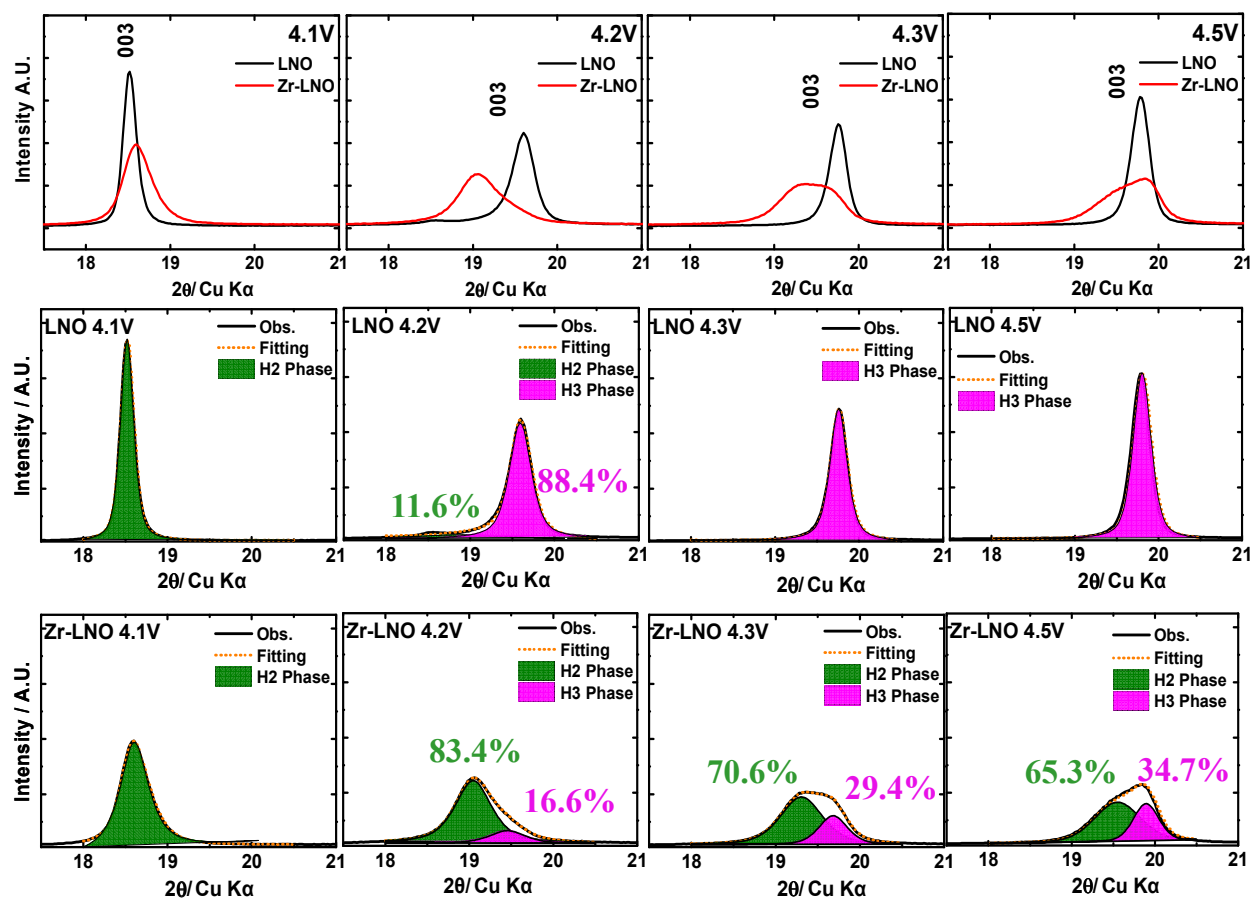
Figure S3. (003) X-ray diffraction (XRD) reflections of the LNO and Zr-LNO cathodes showing the coexistence of the H2 and H3 phases at different charge states (4.1 V, 4.2 V, 4.3 V, and 4.5 V.)
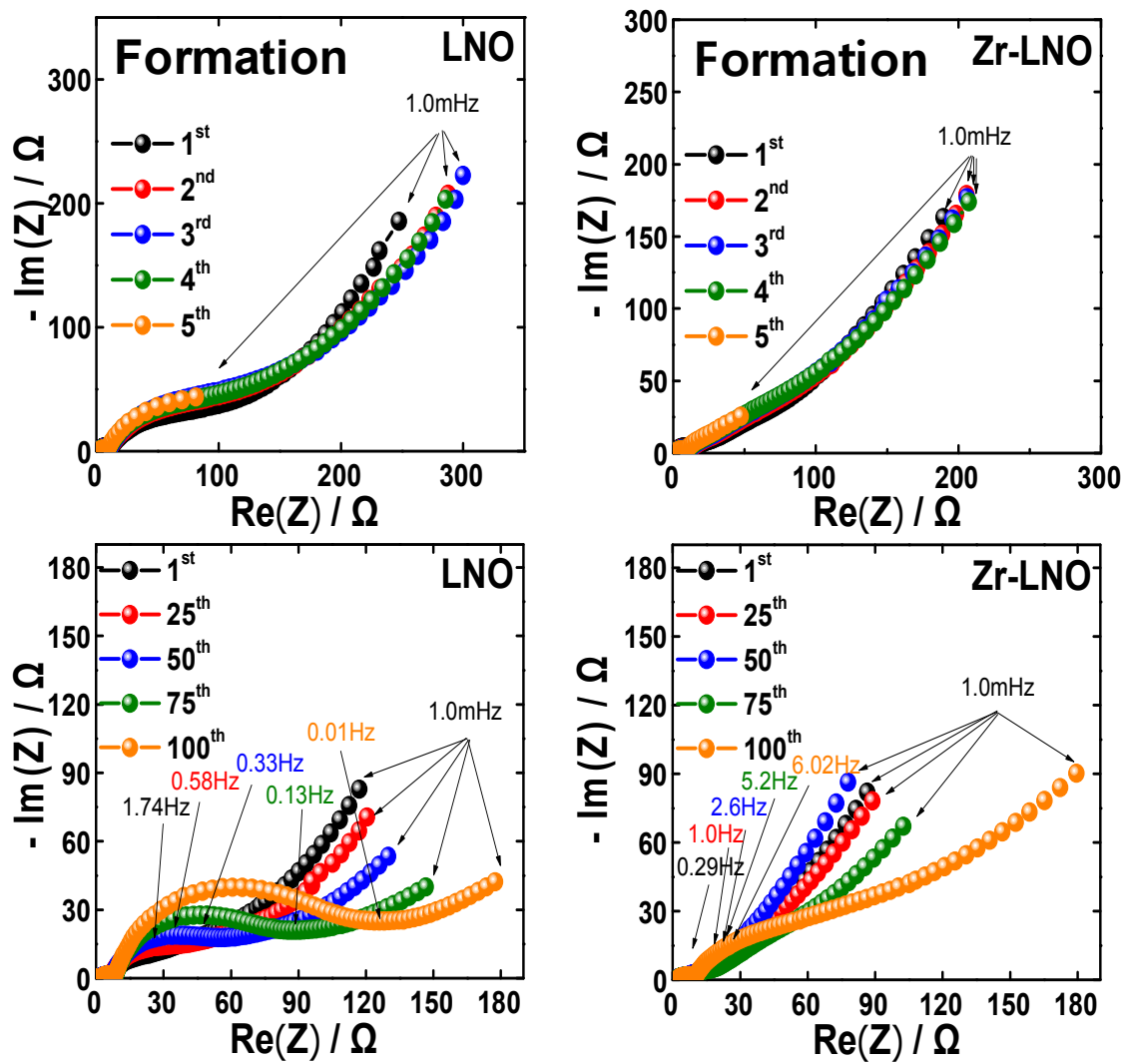
Figure S4. Electrochemical impedance spectroscopy plots of the LNO and Zr-LNO cathodes as a function of the cycle number at the charged state (4.3 V vs. Li/Li$^+$) at 30 °C.
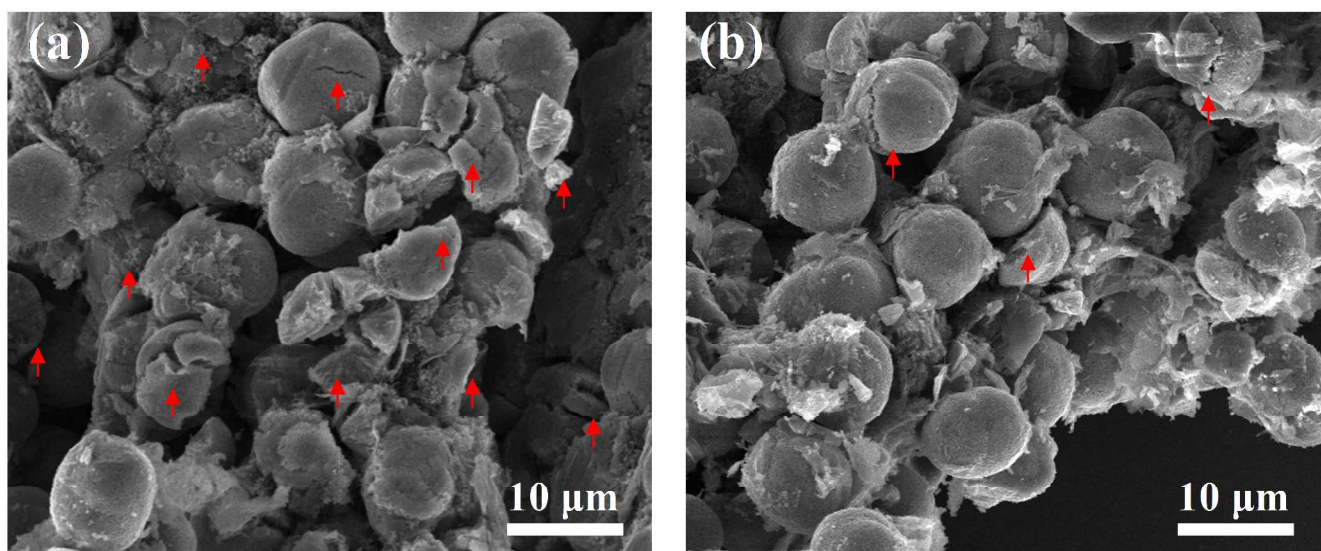
Figure S5. SEM images of the cycled (a) LNO and (b) Zr-LNO cathode after 100 cycles (2.7 - 4.3 V). The SEM image of LNO was cited from Ref. 3, Copyright 2017, The American Chemical Society.
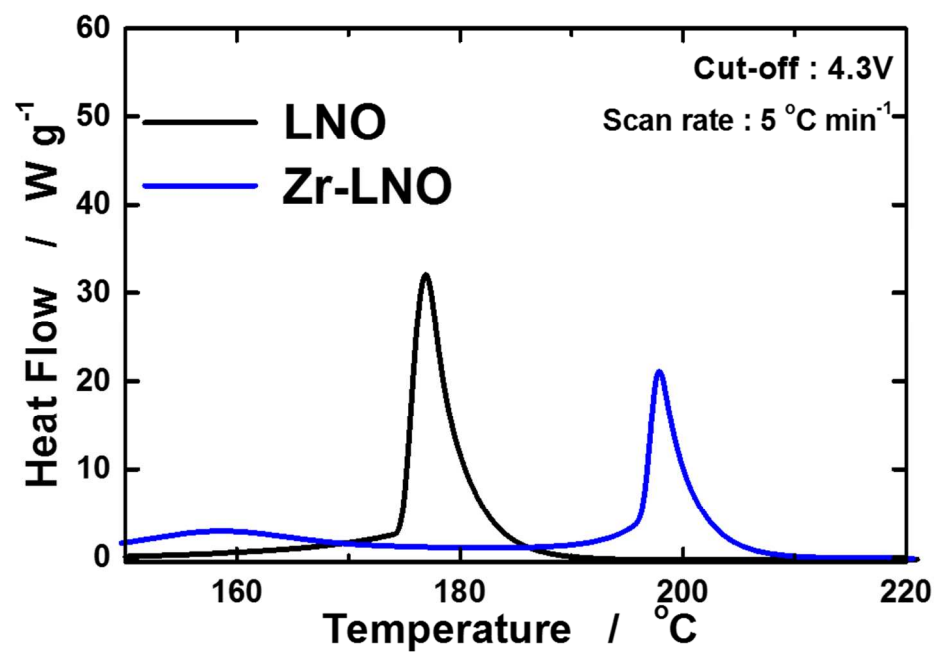
Figure S6. Differential scanning calorimetry (DSC) profiles for the LNO and Zr-LNO cathodes.

Table S1. Lattice parameters of Zr-LNO and LNO obtained from a series of XRD profiles as a function of the first charge state (4.1 V, 4.2 V, 4.3 V, and 4.5 V) in Figure 2c.

Voltage /V	LNO			Zr-LNO		
	a-axis /Å	c-axis /Å	V /Å^3	a-axis /Å	c-axis /Å	V /Å^3
4.1	2.8188(2)	14.3761(1)	98.925(1)	2.8267(9)	14.2978(7)	98.944(1)
4.2	2.8167(1)	14.3061(1)	98.296(1)	2.8219(1)	13.9440(2)	96.162(1)
	2.8143(7)	13.5857(1)	93.192(2)	2.8213(8)	13.6291(8)	93.956(2)
4.3	2.8149(4)	13.5943(2)	93.288(1)	2.8180(6)	13.8323(6)	95.132(2)
				2.8178(4)	13.5688(5)	93.305(2)
4.5	2.8138(2)	13.4634(7)	92.316(3)	2.8169(8)	13.6672(3)	93.925(1)
				2.8151(1)	13.4294(3)	92.167(4)

Table S2. Broad comparison of NCM and NCA layered cathodes. The table illustrates that the proposed Zr-doped LNO layered cathodes clearly outperformed other NCM and NCA layered cathodes reported in the literature.

Num.	Conventional cathode Composition	Voltage Window	Electrolytes	Rate for specific capacity	Cycling rate	Mass loading of AM (mg/cm^2)	Electrode composite Wt% (AM : Conductor : Binder)	Reference
1	NCM 333	3.0-4.3V	1M LiPF$_6$ in EC:DEC (1:1 vol%)	0.1C (20mA/g)	0.5C (100mA/g)	-	85 : 7.5 : 7.5	4
2	NCM 523							
3	NCM 622							
4	NCM 701515							
5	NCM 811							
6	NCM 900505	2.7-4.3V	1.2M LiPF$_6$ in EC:EMC (3:7 vol%) + VC 2wt%					5
7	NCM 952.52.5							
8	LNO							
9	NCA 801505					5	85 : 10 : 5	6
10	NCA 821404							
11	NCA 851104							
12	Zr-LNO					4.5-5	90 : 5.5 : 4.5	This work

All electrochemical evaluations were tested at room temperature.

EC=Ethylene carbonate

DEC= Diethyl carbonate

EMC= Ethyl methyl carbonate

DMC= Dimethyl carbonate

VC= Vinylene carbonate

Reference

(1) Lee, M.-H.; Kang, Y.-J.; Myung, S.-T.; Sun, Y.-K. Synthetic optimization of Li[Ni$_{1/3}$Co$_{1/3}$Mn$_{1/3}$]O$_2$ via co-precipitation. *Electrochim. Acta* **2004**, *50*, 939-948.

(2) Roisnel, T.; Rodriguez-Carvajal, J. *Fullprof Manual*, Institut Laue-Langevin, Grenoble, France **2001**.

(3) Yoon, C. S.; Jun, D.-W.; Myung, S.-T.; Sun, Y.-K. Structural Stability of $LiNiO_2$ Cycled above 4.2 V. *ACS Energy Lett.* **2017**, *2*, 1150-1155.

(4) Noh, H.-J.; Youn, S.; Yoon, C. S.; Sun, Y.-K. Comparison of the structural and electrochemical properties of layered $Li[NixCoyMnz]O2$ (x=1/3, 0.5, 0.6, 0.7, 0.8 and 0.85) cathode material for lithium-ion batteries. *J. Power Sources*. **2013**, *233*, 121-130.

(5) Yoon, C. S.; Choi, M. H.; Lim, B.-B.; Lee, E.-J.; Sun, Y.-K. Review-High-Capacity $Li[Ni_{1-x}Co_{x/2}Mn_{x/2}]O_2$ (x=0.1, 0.05, 0) Cathodes for Next-Generation Li-Ion Battery. *J. Electrochem. Soc*. **2015**, *162*, A2483-A2489.

(6) Yoon, C. S.; Park, K.-J.; Kim, U.-H.; Kang, K. H.; Ryu, H.-H.; Sun, Y.-K. High-Energy Ni-Rich $Li[Ni_xCo_yMn_{1-x-y}]O_2$ Cathodes via Compositional Partitioning for Next-Generation Electric Vehicles. *Chem. Mater.* **2017**, *29*, 10436-10445.